EUROFUSION WPMST1-PR(15) 14452

A.S. Jacobsen et al.

Benchmark and combined velocity-space tomography of fast-ion D-alpha spectroscopy and collective Thomson scattering measurements

Preprint of Paper to be submitted for publication in Plasma Physics and Controlled Fusion

This work has been carried out within the framework of the EUROfusion Consortium and has received funding from the Euratom research and training programme 2014-2018 under grant agreement No 633053. The views and opinions expressed herein do not necessarily reflect those of the European Commission.

1 October 2015

Benchmark and combined velocity-space tomography of fast-ion D-alpha spectroscopy and collective Thomson scattering measurements

A.S. Jacobsen[1], M. Salewski[1], B. Geiger[2], S.B. Korsholm[1], F. Leipold[1], S.K. Nielsen[1], J. Rasmussen[1], M. Stejner, M. Weiland[2] and the ASDEX Upgrade team[2]

[1] Technical University of Denmark, Department of Physics, DK-2800 Kgs. Lyngby, Denmark

[2] Max Planck Institute for Plasma Physics, D-85748 Garching, Germany

E-mail: ajsen@fysik.dtu.dk

Abstract. We demonstrate the combination of fast-ion D-alpha spectroscopy (FIDA) and collective Thomson scattering (CTS) measurements to determine a common best estimate of the fast-ion velocity distribution function by velocity-space tomography. We further demonstrate a benchmark of FIDA tomography and CTS measurements without using a numerical simulation as common reference. Combined velocity-space tomographies from FIDA and CTS measurements confirm that sawtooth crashes reduce the fast-ion phase space densities in the plasma center and affect ions with pitches close to one more strongly than those with pitches close to zero.

1. Introduction

ASDEX Upgrade is equipped with several fast-ion diagnostics providing excellent coverage of the fast-ion velocity space. Collective Thomson scattering (CTS) [1–3] and fast-ion D_α (FIDA) spectroscopy [4–6] are sensitive to fast-ion velocity distribution functions in small measurement volumes. Neutron emission spectroscopy (NES) [7], neutral particle analyzers [8] and gamma-ray spectroscopy (GRS) [9] are sensitive to fast-ion velocity distribution functions along their lines-of-sight. Fast-ion loss detectors are sensitive to ions ejected from the plasma [10].

FIDA measurements can be interpreted using velocity-space tomography [11–13] which has recently been demonstrated experimentally [14] and has since been applied to study sawtooth crashes [6, 15, 16]. Theoretical expectations [17, 18] and previous experiments on TEXTOR using CTS [19] and on DIII-D and ASDEX Upgrade using FIDA [5, 20] indicated that sawteeth eject fast ions with pitches close to one more strongly than those with pitches close to zero from the plasma center. FIDA tomographies of 2D fast-ion velocity distribution functions allow the calculation of the sawtooth-induced redistribution as a function of energy and pitch of the fast ions, confirming the pitch dependence of sawtooth crashes [6, 15, 16]. Simultaneous FIDA tomographies inside and outside the sawtooth inversion radius showed that this decrease of the phase-space densities inside the inversion radius is accompanied by a corresponding increase outside [15]. A reduction fast-ion density above a threshold energy of 10 keV in the plasma center could further be calculated [6].

Here we experimentally demonstrate firstly a method to benchmark and secondly a method to combine different fast-ion diagnostics using simultaneous FIDA and CTS measurements at ASDEX Upgrade. Consistency checks across fast-ion diagnostics are difficult as they observe different regions in position space as well as in velocity space. Consistency has therefore usually been assessed by comparing the measurements with synthetic measurements based on TRANSP/NUBEAM simulations as common reference [2, 21, 22]. Velocity-space tomography allows us to benchmark CTS and FIDA measurements without simulations. Further, we experimentally demonstrate a combination of different fast-ion diagnostics using velocity-space tomography of simultaneous FIDA and CTS measurements [12].

2. Benchmark of FIDA tomography and CTS

In this section we calculate an artificial CTS measurement implied by a FIDA tomography and compare it with the actual CTS measurement in discharge 30382 [23]. The discharge was heated by neutral beam injector Q3 at 60 keV in deuterium and 2.5 MW. Figure 1 shows an overview of main parameters. Figure 2 shows simultaneously acquired spectra in four FIDA views before and after the large sawtooth crash at $t = 2.29$ s. The measurement volumes of the four FIDA views are at yy within zz cm. We reject spectral ranges dominated by beam emission or impurity lines or if they are sensitive to ions below 10 keV or only to ions above 100 keV as shown in figure 2. As the NBI was not modulated, a standard subtraction of background noise and impurity lines in the FIDA spectra is not possible. Therefore some wavelength ranges are not usable here. The low density ($n_e = 3 \times 10^{19}\mathrm{m}^{-3}$) makes up for this shortcoming due to the resulting significantly improved signal-to-noise ratio of the FIDA measurements. The sawtooth crash leads to reductions in FIDA measurements.

Figure 3 shows FIDA tomographies before and after the sawtooth crash as calculated from the FIDA spectra in figure 2 using the minimum Fisher information regularization on a 15×15 grid [16]. The FIDA spectra depend not only on the fast ion phase-space density but also on nuisance parameters such as the electron density which can themselves have sawtoothing time traces. FIDA tomographies account for any changes in nuisance parameters. The FIDA tomographies allow the computation of 1D velocity-distribution functions $g(u)$ which are artificial CTS measurements implied by FIDA tomography. These artificial CTS measurements are shown together with the actual CTS measurements before and after the sawtooth crash in figure 4. The CTS measurements include the injected fast ions as well as the fast ions found in the tails of the thermal ion distribution. The artificial CTS measurements match the actual CTS

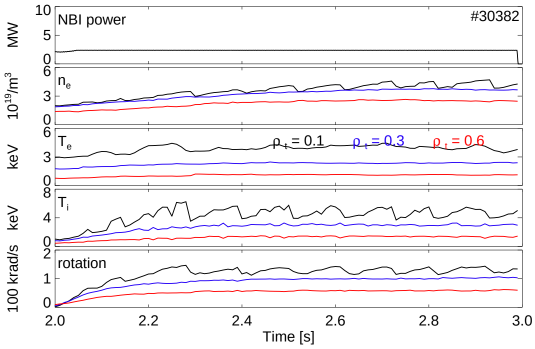

Figure 1. Overview of discharge 30382 showing the NBI power, electron density, electron temperature, ion temperature and plasma rotation.

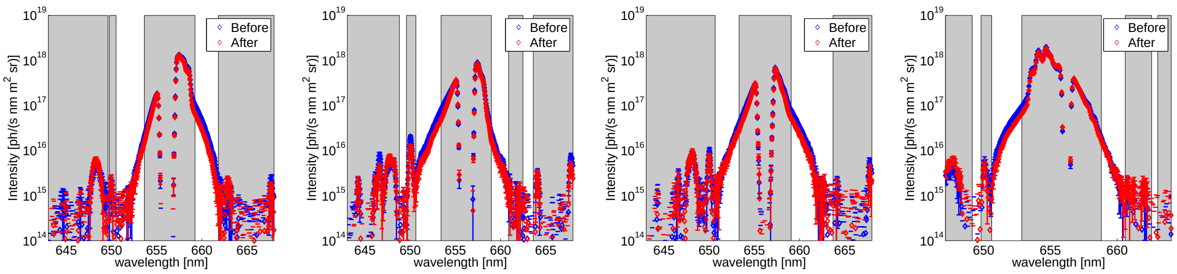

(a) (b) (c) (d)

Figure 2. Simultaneously measured FIDA spectra in four views before and after a sawtooth crash at $t = 2.29$ s in discharge #30382. The shaded regions are rejected.

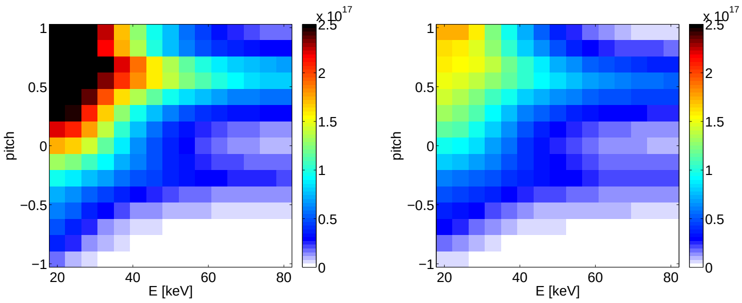

(a) Before (b) After

Figure 3. FIDA tomographies of the 2D fast-ion distribution function [ions/m^3/keV] before and after a sawtooth crash at $t = 2.29$ s in discharge #30382 based on the spectra from figure 2.

measurements quite well in overall shape. However, the artificial CTS measurements lie slightly above the actual CTS measurements. A possible explanation is that the FIDA measurement volume is slightly more central than the CTS measurement volume. The CTS measurement volume is located at $(R, z) = (1.62, 0.06)$ m. Hence the fast-ion density as well as bulk ion densities and temperatures are slightly larger in the FIDA measurement volume.

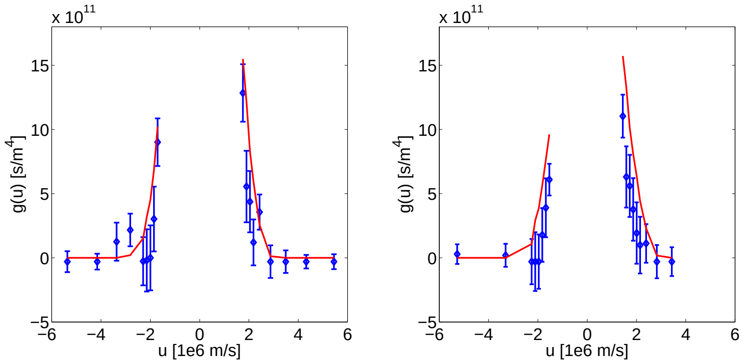

(a) pre (b) post

Figure 4. Comparison of real CTS measurements and artificial CTS measurements implied by FIDA tomographies in figure 3.

3. Combination of CTS and FIDA in velocity-space tomography

Velocity-space tomography allows us to combine measurements taken with different fast-ion diagnostics to calculate a common best estimate of the fast-ion distribution function [12]. Here we present an experimental demonstration. For such a combination, the normalization of the measurements and of the transfer matrix with the estimated uncertainties becomes crucial [12]. These uncertainties need to be defined consistently across the different diagnostics. CTS uncertainties account for uncertainties in the measured spectral power densities as well as in the nuisance parameters used in the fit of $g(u)$ [**?**, 1, 3]. Uncertainties in FIDA intensities can be calculated based on the photon noise. However, the uncertainties in the nuisance parameters are not often accounted for as they do not influence the measured FIDA intensity but the synthetic FIDA measurement based on TRANSP. Here we need to account for these uncertainties to treat FIDA and CTS on an equal footing. They enter the problem as uncertainty in the weight functions. The FIDA weight functions are most sensitive to the electron temperature and density, the ion temperature and drift velocity and the effective charge. Here we estimate the uncertainty due to these nuisance parameters as demonstrated in reference [16].

Figure 5 shows tomographies based on combined FIDA and CTS measurements before and after the sawtooth crash together with a corresponding TRANSP simulation. We neglect the small difference in the spatial locations of the measurement volumes. We further show the measured and simulated relative crash sizes resolved in velocity space. The tomographies confirm previous results based on FIDA tomographies [6, 15, 16]. The fast-ion density is strongly reduced. This reduction is stronger for pitches close to one than for pitches close to zero. The pitch dependence of the sawtooth crash is much weaker in the simulation compared with the measurements. Figure 6 shows the estimated uncertainty of the measurement based on uncertainties in the tomographies and standard error propagation. The uncertainties represent photon noise, model uncertainty and reconstruction uncertainty. The tomographies are reliable for positive pitch and energies below the injection energy as well as for negative pitches at somewhat lower energies.

A comparison of figure 5(a)–(b) and figure 3 shows that the addition of CTS measurement does not change the tomographies appreciably. This is here expected for three reasons. Firstly, the FIDA measurements consist of 487 usable data points while the CTS measurements consist of 18. In the future the number of CTS measurements could be significantly increased by using high frequency resolution CTS measurements which have so far been restricted to thermal rather than fast ions [24]. Secondly, the uncertainty in FIDA measurements is about 5% of the total signal whereas the uncertainty of CTS measurements is about 20%. This discharge has a rather low density leading to the relatively large signal-to-noise ratio of the FIDA measurements. As we have about 20 times more usable FIDA data points, this choice of density yields the best result for the combined tomography but in other discharges the signal-to-noise ratio of CTS and FIDA might become more similar. Thirdly, the reasonable matches between the FIDA-implied artificial CTS measurements and the actual CTS measurements suggest that the CTS measurements agree with the FIDA tomography and thus should not change it much.

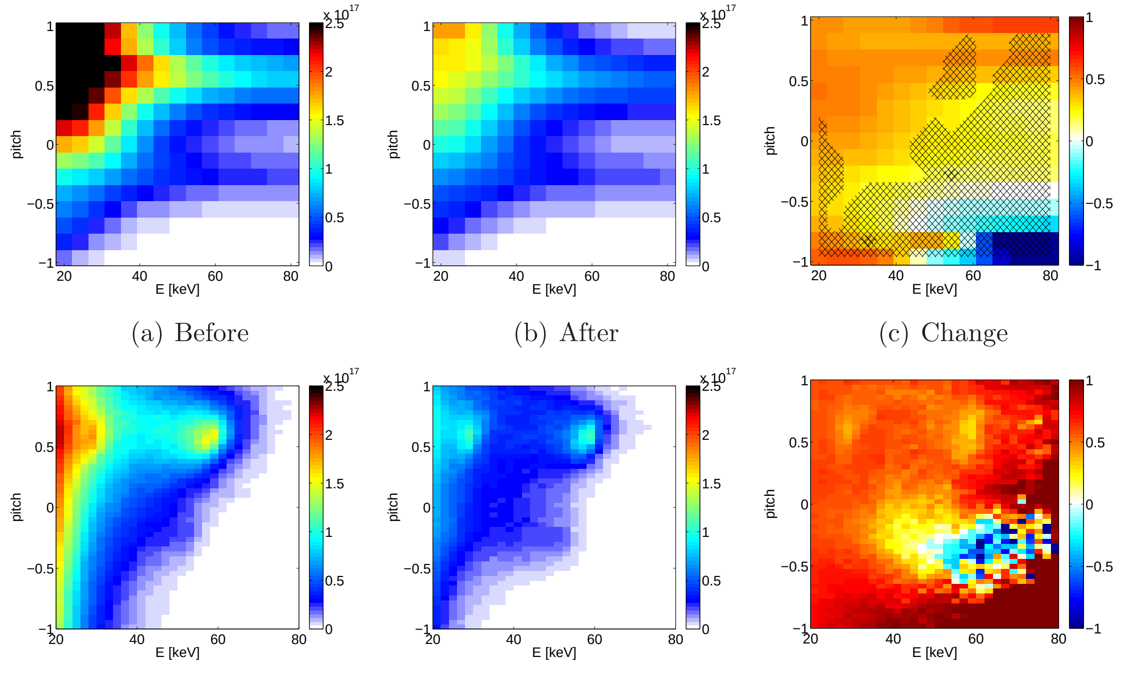

(a) Before (b) After (c) Change

(d) TRANSP before (e) TRANSP after (f) TRANSP change

Figure 5. Velocity-space tomographies [ions/m^3/keV] from combined FIDA and CTS measurements before and after a sawtooth crash as well as the relative change. The lower row shows corresponding TRANSP simulations. In the hatched area in (c) the uncertainties on the relative change (see figure 6) are larger than the relative change.

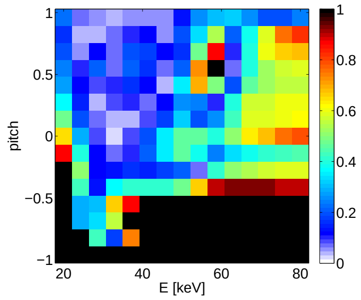

Figure 6. Uncertainty of the relative crash size based on velocity-space tomographies before and after the sawtooth crash. Regions with large uncertainties compared with the crash size are shown as hatched regions in figure 5.

4. Discussion and Conclusions

We have experimentally demonstrated that FIDA measurements in four views and CTS measurements in one view can be combined to give a common best estimate of the 2D fast-ion distribution function using velocity-space tomography. We further benchmarked CTS and FIDA without the need for fast-ion simulations as common reference. Our methods apply directly to LHD which is equipped with CTS [25] and two FIDA views [26]. Our approach relies on weight functions for FIDA [21, 27] and CTS [28]. The recently derived NES weight functions [29] will allow us to combine FIDA and CTS with NES in a 3D inference with a spatial coordinate as third dimension. The availability of six FIDA views and two CTS views will further improve the inversion for studies of for example Alfvén eigenmodes or fast-ion distributions from ion cyclotron resonance heating. Our approach will together with recently derived GRS weight functions [30] allow us to combine GRS and NES measurements at JET in velocity-space tomography of fusion alphas in the upcoming JET D-T campaign. Lastly, ITER will be equipped with GRS, NES and CTS diagnostics. A helium variant of FIDA could provide additional measurements. Thus, the methods of benchmarking and combination of fast-ion diagnostics experimentally demonstrated here will directly apply to ITER. We demonstrated our approach by benchmarking and combining FIDA and CTS measurements before and after a sawtooth crash at ASDEX Upgrade. Previous results of the crash size and the velocity-space resolved ejection of fast ions from the center based on FIDA tomography could be confirmed [5, 15, 16].

Acknowledgments

This work has been carried out within the framework of the EUROfusion Consortium and has received funding from the Euratom research and training programme 2014-2018 under grant agreement No 633053. The views and opinions expressed herein do not necessarily reflect those of the European Commission.

References

[1] Salewski M *et al* 2010 *Nucl. Fusion* **50** 035012
[2] Rasmussen J *et al* 2015 *Plasma Phys. Control. Fusion* **57** 075014
[3] Nielsen S K *et al* 2015 *Plasma Phys. Control. Fusion* **57** 035009
[4] Geiger B *et al* 2011 *Plasma Phys. Control. Fusion* **53** 065010
[5] Geiger B *et al* 2015 *Plasma Phys. Control. Fusion* **57** 014018
[6] Geiger B *et al* 2015 *Nucl. Fusion* **83** 083001
[7] Tardini G *et al* 2012 *Journal of Instrumentation* **7** C03004–C03004
[8] Schneider P A *et al* 2015 *Rev. Sci. Instrum.* **86** 073508
[9] Nocente M *et al* 2012 *Nucl. Fusion* **52** 094021
[10] García-Muñoz M *et al* 2007 *Nucl. Fusion* **47** L10–L15
[11] Salewski M *et al* 2012 *Nucl. Fusion* **52** 103008
[12] Salewski M *et al* 2013 *Nucl. Fusion* **53** 063019
[13] Salewski M *et al* 2015 *Plasma Phys. Control. Fusion* **57** 014021
[14] Salewski M *et al* 2014 *Nucl. Fusion* **54** 023005
[15] Weiland M *et al* 2016 *submitted* Velocity space resolved fast–ion measurements from five FIDA views at the tokamak ASDEX Upgrade
[16] Jacobsen A S *et al* 2016 *submitted* Inversion methods for fast–ion velocity–space tomography in fusion plasmas
[17] Kolesnichenko Y *et al* 2000 *Nuclear Fusion* **40** 1325–1341
[18] Jaulmes J *et al* 2015 *14^{th} IAEA Technical Meeting on Energetic Particles*
[19] Nielsen S K *et al* 2011 *Nucl. Fusion* **51** 063014
[20] Muscatello C M *et al* 2012 *Plasma Phys. Control. Fusion* **54** 025006
[21] Heidbrink W W *et al* 2007 *Plasma Phys. Control. Fusion* **49** 1457–1475
[22] Heidbrink W W *et al* 2014 *Plasma Phys. Control. Fusion* **56** 095030
[23] Rasmussen J *et al* 2015 *14^{th} IAEA Technical Meeting on Energetic Particles*
[24] Stejner M *et al* 2015 *Plasma Phys. Control. Fusion* **57** 062001
[25] Nishiura M *et al* 2014 *Nucl. Fusion* **54** 023006
[26] Ito T *et al* 2010 *Rev. Sci. Instrum.* **81** 10D327
[27] Salewski M *et al* 2014 *Plasma Phys. Control. Fusion* **56** 105005
[28] Salewski M *et al* 2011 *Nucl. Fusion* **51** 083014
[29] Jacobsen A S *et al* 2015 *Nucl. Fusion* **55** 053013
[30] Salewski M *et al* 2015 *Nuclear Fusion* **55** 093029